Medicago truncatula DNF2 is a PI-PLC-XD-containing protein required for bacteroid persistence and prevention of nodule early senescence and defense-like reactions

Marie Bourcy[1], Lysiane Brocard[1], Catalina I. Pislariu[2], Viviane Cosson[1], Peter Mergaert[1], Millon Tadege[2], Kirankumar S. Mysore[2], Michael K. Udvardi[2], Benjamin Gourion[1] and Pascal Ratet[1]

[1]Institut des Sciences du Végétal, CNRS, Avenue de la terrasse, 91198, Gif Sur Yvette, France; [2]The Samuel Roberts Noble Foundation, 2510 Sam Noble Parkway, Ardmore, 73401, OK, USA

Summary

- *Medicago truncatula* and *Sinorhizobium meliloti* form a symbiotic association resulting in the formation of nitrogen-fixing nodules. Nodule cells contain large numbers of bacteroids which are differentiated, nitrogen-fixing forms of the symbiotic bacteria. In the nodules, symbiotic plant cells home and maintain hundreds of viable bacteria. In order to better understand the molecular mechanism sustaining the phenomenon, we searched for new plant genes required for effective symbiosis.
- We used a combination of forward and reverse genetics approaches to identify a gene required for nitrogen fixation, and we used cell and molecular biology to characterize the mutant phenotype and to gain an insight into gene function.
- The symbiotic gene *DNF2* encodes a putative phosphatidylinositol phospholipase C-like protein. Nodules formed by the mutant contain a zone of infected cells reduced to a few cell layers. In this zone, bacteria do not differentiate properly into bacteroids. Furthermore, mutant nodules senesce rapidly and exhibit defense-like reactions.
- This atypical phenotype amongst Fix⁻ mutants unravels *dnf2* as a new actor of bacteroid persistence inside symbiotic plant cells.

Introduction

Most species of the legume family are able to form symbiotic associations with nitrogen-fixing soil bacteria, commonly referred to as rhizobia. These associations result in the development of a specialized organ of the root system, called the nodule, in which the bacteria invade the symbiotic plant cells. The early steps of the nodulation process have been studied extensively in the model legumes *Medicago truncatula* and *Lotus japonicus*. The very early steps of the plant–microbe interaction are highly similar in these two models; the genes and molecules involved in the reciprocal recognition of the two symbiotic partners are largely conserved (Oldroyd *et al.*, 2011). The interaction starts with the exudation of flavonoids by the plant roots. These molecules are secondary metabolites recognized by the bacteria. In response, the rhizobia synthesize nodulation factors, called Nod factors, which are perceived in a host-specific manner by the plant to initiate the symbiotic process. At the root surface, root hairs curl to surround attached bacteria. These entrapped bacteria induce invagination of the plasma membrane and the formation of a progressing structure, called the infection thread, in which bacteria develop towards the root cortex. Nod factors trigger cortical cell dedifferentiation and the initiation of a nodule primordium. Infection threads reaching the primordium release bacteria within

the plant cells. At this stage, nodule formation diverges between *Medicago* and *Lotus*. In *Medicago*, distal primordium cells will not become infected with rhizobia and will develop into an apical nodule meristem (Timmers *et al.*, 1999). Persistence of the meristem results in continuously growing, indeterminate nodules. By contrast, the primordia formed on *Lotus* plants will not form a meristem, and therefore these nodules are of the determinate type.

Persistence of the apical meristem in indeterminate nodules of *Medicago* results in nodules harboring different cell types organized in zones (Vasse *et al.*, 1990). The apical meristematic zone, or zone I, contains constantly dividing plant cells that ensure nodule growth (Timmers *et al.*, 1999). In the infection zone, zone II, bacteria are released from the infection threads and invade the plant cells. The rhizobia and their surrounding plant-derived membrane form the symbiosomes. Within the symbiosomes, the bacteria undergo a morphological terminal differentiation involving cell elongation and genome amplification, a process which is governed by numerous plant nodule-specific cysteine-rich peptides, the so-called NCR peptides, which are addressed to the bacterium-containing compartments (Van de Velde *et al.*, 2010). In the interzone II–III, bacteria fully differentiate into nitrogen-fixing bacteroids. In the fixation zone III, the bacteroids reduce atmospheric nitrogen and transfer the resulting

ammonium to the plant cells (Vasse *et al.*, 1990). Zone IV, also called the senescence zone, is formed in older nodules and is characterized by the degeneration of both the host cells and their bacteroids. A recent study has indicated that leaf senescence markers, such as cysteine proteinases, are induced in this zone (Van de Velde *et al.*, 2006). The proximal zone V is characterized by the presence of saprophytic rhizobia which proliferate in the remains of the cells after their senescence (Timmers *et al.*, 2000).

In *M. truncatula*, several genes involved in the first steps of the interaction, Nod factor signaling and the immediate downstream events have been described (Oldroyd *et al.*, 2011). Far less is known in this model organism about the genes involved in the subsequent steps of the symbiotic process, once bacteria have been released into the plant cell cytoplasm. This contrasts with the knowledge acquired on other legume organisms, especially on *L. japonicus*, in which genes such as *LjIGN1*, *FEN1* and *SEN1* have been cloned and described (Kumagai *et al.*, 2007; Hakoyama *et al.*, 2009, 2012). In *Lotus*, bacteroids do not undergo terminal differentiation; thus, the study of *Medicago* mutants altered in these symbiotic steps is also of particular interest to understand the role of terminal differentiation. Starker *et al.* (2006) identified eight *M. truncatula* mutants altered in their capacity to support nitrogen fixation, that are, Fix$^-$ mutants (see also Mitra & Long, 2004). These mutants clustered into seven complementation groups and the corresponding genes were designated as *dnf1* to *dnf7*, where dnf stands for *d*oes *n*ot *f*ix nitrogen. Microarray experiments were performed on *dnf1*, *2* and *7*, and the expression of nodulation markers was studied in all of them (Mitra & Long, 2004; Starker *et al.*, 2006). Of the seven mutated genes involved in nitrogen fixation, only *DNF1* has been cloned so far (Wang *et al.*, 2010). This gene encodes a signal peptidase subunit required to target NCR peptides to the symbiosomes (Van de Velde *et al.*, 2010).

In recent years, ambitious projects have been developed to produce genomic resources useful for the study of the *M. truncatula–Sinorhizobium meliloti* symbiosis. Amongst these are extensive transcriptomic data (El Yahyaoui *et al.*, 2004; Van de Velde *et al.*, 2006; Benedito *et al.*, 2008; Maunoury *et al.*, 2010; Moreau *et al.*, 2011), large insertional mutant collections (Tadege *et al.*, 2008; Iantcheva *et al.*, 2009; Cheng *et al.*, 2011), developed thanks to the establishment of mutagenesis protocols (d'Erfurth *et al.*, 2003; Rakocevic *et al.*, 2009), and the recently published *M. truncatula* genome sequence (Young *et al.*, 2011).

We made use of these resources to identify a symbiotic plant gene, *DNF2*, and we demonstrate its involvement in the nitrogen fixation process. Phenotypes of knockout mutants were examined, and we showed that this gene is required for symbiosome persistence, to prevent plant defense reactions and to avoid early nodule senescence.

Materials and Methods

Bacterial strains and inoculation

The *S. meliloti* strains used in this study, including Sm1021 (Meade *et al.*, 1982), Rm41 (Kondorosi *et al.*, 1984) and Sm2011 (Rosenberg *et al.*, 1981), and their derivatives (Leong

et al., 1985; Ardourel *et al.*, 1994; Penmetsa & Cook, 1997), were cultivated at 30°C in YTB (Orosz *et al.*, 1973) or YEB (Krall *et al.*, 2002) medium supplemented with 0.5 mg.ml^{-1} of streptomycin for Sm1021 and with 0.01 mg.ml^{-1} of tetracycline for the strains harboring the pXLGD4 plasmid. To prepare plant inoculum, fresh liquid cultures were washed twice with sterile distilled water and the optical density at 600 nm (OD$_{600\,nm}$) of the suspensions was adjusted to 0.1.

Plant material

All *M. truncatula* plants used in this study were from the R108 ecotype (Hoffmann *et al.*, 1997), except for the Jemalong *dnf2* mutant (Mitra & Long, 2004; Starker *et al.*, 2006). The *Tnt1* insertion mutant lines were generated at the Noble Foundation (Tadege *et al.*, 2008). The *MERE1* insertion mutant line MS240 corresponds to a somaclonal variant obtained by regeneration of a T-DNA-tagged *Medicago* line (Scholte *et al.*, 2002; Brocard *et al.*, 2006; Rakocevic *et al.*, 2009). For expression studies using the β-glucuronidase reporter gene, transgenic plants expressing a *DNF2* promoter::*gus* fusion (pMB132 construct, see later) were generated by *Agrobacterium tumefaciens* strain EHA105 transformation of *M. truncatula* R108, as described in Cosson *et al.* (2006). Of the eight independent transgenic plants tested, two did not express the reported gene and six expressed it specifically with the same expression pattern in the nodules. One of these transgenic lines was used for further studies.

Seeds were surface sterilized and germinated as described in the *Medicago truncatula Handbook* (Garcia *et al.*, 2006; www.noble.org/MedicagoHandbook). For seed production or crosses, plants were cultivated in the greenhouse under long-day conditions (16-h light : 8-h dark cycle) at 24°C, 50% humidity. For the segregation study, 25 plants of the mutant line NF0217 were grown in the greenhouse on a mixture of sand and perlite (1/3, v/v) and watered with nitrogen-free 'i' medium (www.isv.cnrs-gif.fr/embo01/manuels/pdf/module1.pdf) to allow nodulation. Seedlings were inoculated with 10 ml of an *S. meliloti* suspension prepared as described above.

For *in vitro* nodulation experiments, seedlings were transferred onto square plates filled with Buffered Nodulation Medium (Ehrhardt *et al.*, 1992) supplemented with 0.1 μM AVG [L-α-(2-aminoethoxyvinyl)-Gly]. The plates were then incubated in growth chambers (16-h light : 8-h dark cycle, 24°C). After 1 or 2 days, each plant root was inoculated with 50 μL of bacterial suspension. Acetylene reduction assays were conducted on plants at 27 days post-inoculation (dpi) as described in Hardy *et al.* (1968).

PCR reverse screening for *Tnt1* and *MERE1* insertion mutants in the *MTR_4g085800* gene

Plant genomic DNA was extracted from leaves as described by d'Erfurth *et al.* (2003). *Medicago truncatula* Fix$^-$ mutant lines available in our laboratory were screened for the presence of insertion in *MTR_4g085800* by PCR. Genomic DNA was tested in PCRs using three primers per reaction. Two primers

correspond to the external parts of the retrotransposon (*Tnt1* or *MERE1*), called LTR for Long Terminal Repeat: primers LTR4 and LTR6 for *Tnt1* or MERE1 and MERE4 for *MERE1*. The third primer was specific to the *MTR_4g085800* gene and hybridizes either to the start or the stop codon region for the forward and reverse primer, respectively. All primers are listed in Supporting Information Table S1.

Expression studies

Total RNA was extracted from plant organs using the RNeasy Plant Mini Kit (Qiagen, http://www.qiagen.com/). For cDNA synthesis, RNA samples were treated with RNase-free DNAse I to remove traces of genomic DNA. Reverse transcription (RT) was then performed from 1 μg of total RNA using a poly-T primer and the First Strand cDNA Synthesis Kit from Fermentas (http://www.fermentas.de). Quantitative RT-PCRs were performed using the LightCycler® FastStart DNA Master SYBR Green I Kit on a LightCycler® 480 machine according to the manufacturer's instructions (Roche, http://www.roche.com). Primers are listed in Table S1. The PCR conditions were as follows: 95°C for 10 min (one cycle); 95°C for 5 s, 60°C for 5 s and 72°C for 15 s (40 cycles). PCR amplification specificity was verified using a dissociation curve (55–95°C). Two biological replicates were analyzed. The *RBP1* gene was used as a constitutive control for the quantitative RT-PCR (Lelandais-Briere *et al.*, 2009).

For the *in situ* expression study, a Gateway vector harboring a 4-kb DNA fragment corresponding to the upstream sequence of the *DNF2* start codon was used. This vector, derived from pMDC163, was kindly supplied by Dr Dong Wang (Stanford University, Stanford, CA, USA). The site resulting from L/R recombination between the β-glucuronidase AUG and the 5′ UTR of the *DNF2* gene was removed by digestion with the enzymes *Sph*I and *Asc*I. The fusion was restored by ligation of an adaptor generated with primers Fusprom1 and Fusprom2 (Table S1) into the linearized vector, resulting in the pMB132 vector.

For the study of alternative splicing variants, cDNAs were cloned into pGEM-T Easy (Promega) after amplification using primers 4-1/4-3, 2-b/4-3, AUG/4-3, 2-d/ex5-6 (Table S1), and then sequenced.

Microscopy

Thin sections (7 μm) of Technovit-embedded nodules were prepared as described by Van de Velde *et al.* (2006) and stained with 0.02% toluidine blue. Semi-thin sections (50–70 μm) of 6% agarose-embedded nodules were prepared, and β-galactosidase and β-glucuronidase activities were revealed, as described in Boivin *et al.* (1990) and Welchen & Gonzalez (2005), respectively. X-Gal-stained nodules were first fixed in 2.5% glutaraldehyde in 0.1 M PIPES (piperazine-N,N'-bis(2-ethanesulfonic acid)), pH 7.2. Sections in Fig. 3 were observed and photographed with a Leica DMI 6000B inverted microscope, and sections in Fig. 6 were observed and photographed with an Olympus BX41 epifluorescence microscope using transmitted light for the bright field picture and fluorescent light from the BrightLine GFP

filter set EX47 (Hitschfel Instruments, Inc., St. Louis, Missouri, USA).

Free-living rhizobia and bacteroids extracted from nodules were stained with 4′,6′-diamidino-2-phenylindole (DAPI, 5 μg.ml^{-1}) and observed by fluorescence microscopy, as described by Mergaert *et al.* (2006).

The LIVE/DEAD® BacLight Bacterial Viability Kit was used as described by Haag *et al.* (2011). Briefly, immediately after slicing, semi-thin sections (80 μm) of 6% agarose-embedded nodules were stained for 20 min in a mixture of Syto9 (3.34 mM) and propidium iodide (20 mM). In addition to nuclei, propidium iodide stains only bacteria with compromised membrane integrity. Sections were then briefly rinsed in distilled water and observed on a Leica TCS SP2 inverted confocal microscope under appropriate illumination, as described by Haag *et al.* (2011).

Phenolic compounds were revealed by potassium permanganate staining, as described previously (Vasse *et al.*, 1993). Freshly sliced agarose-embedded nodule sections were subjected to postfixation in 0.04% KMnO$_4$, 10 mM PIPES, pH 7.2, for 1 h at room temperature. Sections were rinsed with 10 mM PIPES, pH 7.2, and subsequently stained in 0.01% methylene blue for 10 min. Stained sections were cleared briefly in bleach (2.4% active chloride), rinsed with water and photographed using bright-field microscopy.

For the electron microscopy study, wild-type (WT) and MS240 nodules were dissected from the root system and cut longitudinally to improve the infiltration process. Nodules were placed in a fixation solution of 1.5% paraformaldehyde and 3% glutaraldehyde in 100 mM phosphate buffer (pH 6.8). Nodules were vacuum infiltrated with the fixation solution twice for 10 min, followed by four times for 5 min, and further fixed for 1 h under gentle shaking at room temperature. Samples were subsequently rinsed four times for 10 min with 100 mM phosphate buffer. The nodules were stained for 1 h with 1% tannic acid in 100 mM phosphate buffer and rinsed four times for 10 min with 100 mM phosphate buffer. They were then subjected to post-fixation with 0.1% OsO$_4$ in 100 mM phosphate buffer for 45 min at room temperature. After rinsing 10 times for 5 min with distilled water, nodules were dehydrated in a series of increasing ethanol concentrations (20%, 30%, 50%, 70%, 85%, 90% and 100%) at 4°C. Propylene oxide was used as a transition solvent before Epon 812 (Electron Microscopy Sciences, Hatfield, Pennsylvania, USA) infiltration. Samples were polymerized in Epon 812 at 60° C for 24 h. Sections were obtained using a Reichert Depew, New York, USA ultramicrotome EM UCS (electron microscopy ultracut S). To localize zones II and III precisely, thick longitudinal nodule sections (500 nm) stained with toluidine blue were observed with a light microscope. The distance between the zone of interest and the edge of the block was evaluated using ImageJ software. After turning the block 90° and trimming the excess of resin to reach the zone of interest, transverse thin sections (70 nm) were obtained and observed with an FEI (Hillsboro, Oregon, USA) CM10 electron microscope. Images were recorded with an XR60 CCD camera (AMT, Woburn, Massachusetts, USA) at 80 kV.

Flow cytometry

Flow cytometry measurements of ploidy levels in nodule cell nuclei were performed as described previously (Cebolla *et al.*, 1999). For each experiment, 11 nodules from five plants at 28 dpi were pooled, and each experiment was repeated twice. The mean values of the repetitions were calculated. The fractions of nuclei at ploidy levels from 2 to 64°C were expressed as a percentage of the total number of nuclei measured. The endoreduplication index (EI), expressing specifically the levels of 16, 32 and 64°C endoreduplicated nuclei, was calculated as described previously (Maunoury *et al.*, 2010). Bacteroids were extracted from nodules (Mergaert *et al.*, 2006), and stained with DAPI (5 µg ml^{-1}). Measurements were performed with a Beckman-Coulter (Danvers, Massachusetts, USA) ELITE ESP flow cytometer.

Results

A candidate symbiotic gene identified using *Medicago* genomics resources

The Fix$^-$ mutant NF0217 was identified during a screen of the *M. truncatula Tnt1* mutant collection at the Noble Foundation (Tadege *et al.*, 2008; Pislariu *et al.*, 2012). Flanking sequence tags (FSTs) corresponding to the *Tnt1* insertion sites were available

for this line (http://bioinfo4.noble.org/mutant/index.php). The expression profiles of the *Tnt1*-tagged genes were analyzed using the *M. truncatula* gene expression atlas (MtGEA; Benedito *et al.*, 2008; He *et al.*, 2009; http://mtgea.noble.org/v2/index.php). Of the 35 genes tagged by *Tnt1* in NF0217, only *MTR_4g085800* (Fig. 1a) is exclusively expressed in nodules. Relative expression levels of probeset Mtr.630.1.S1_at corresponding to *MTR_4g085800* in different organs and during nodulation are presented in Fig. 1(b). The genomic sequence of *MTR_4g085800* is 2084 bp long from the predicted start to the stop codon. According to the sequences available in public databases, this gene is composed of eight exons (Fig. 1a), which together form the TC119183 cDNA sequence. In NF0217, *Tnt1* is inserted in the sixth exon, 1487 bp downstream of the AUG start codon (FST NF0217Ase4; Fig. 1a). The predicted 334-amino-acid protein encoded by TC119183 displays a signal peptide and a phosphatidylinositol-specific phospholipase C X domain (PI-PLCXD; Fig. S1). It belongs to a protein family that is widespread in plants, with multiple genes in each species, including *M. truncatula*. Despite the presence of the PI-PLCXD, members of this family differ from canonical PI-PLC by lacking the other PI-PLC functional domains. The family includes proteins of *Arabidopsis thaliana*, *Phaseolus vulgaris* and *Glycine max*, as well as a *Lotus japonicus* nodulin of unknown function (LJNUF; AB167409.1; Kinoshita *et al.*, 2004; Fig. S1).
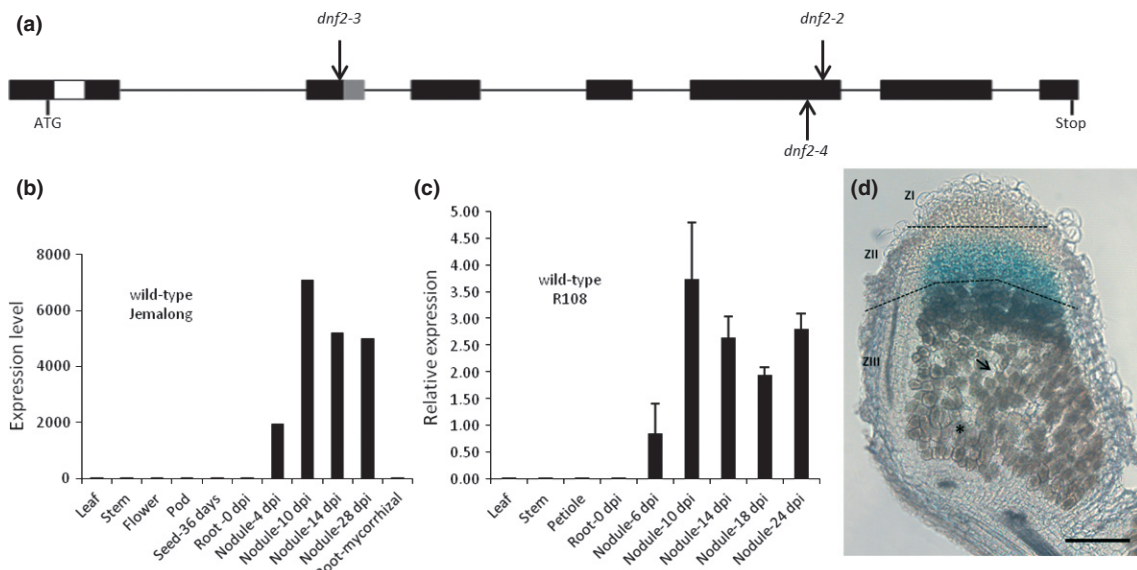

Fig. 1 *DNF2* gene structure and nodule-specific gene expression. (a) The *DNF2* (*MTR_4g085800*) gene contains eight exons represented by black boxes. The gray area in the 3′ part of the third exon contains four alternative splicing sites (see Supporting Information Fig. S5). The first intron that can be retained in one splicing form is represented by a white box and all other introns are represented by black lines. The positions of *Tnt1* and *MERE1* insertions corresponding to the three dnf2 mutant lines NF0217 (*dnf2-2*), NF2496 (*dnf2-3*) and MS240 (*dnf2-4*) are indicated by black arrows (top, *Tnt1* insertion; bottom, *MERE1* insertion). (b) *DNF2* expression profile in organs of wild-type plants from the Jemalong ecotype. Data were extracted from the MtGEA database (http://mtgea.noble.org). dpi, days post-inoculation. (c) Expression levels of *DNF2* in different organs and during nodule formation on wild-type R108 *Medicago truncatula* plants. Plants were inoculated with the *Sinorhizobium meliloti* strain Rm41. Transcript levels were determined by quantitative reverse transcription-polymerase chain reaction (qRT-PCR) and normalized using *RBP1*. Two biological replicates, one with two technical replicates, were analyzed. The error bars represent the standard error. (d) Section of a 17-dpi nodule developed on an R108 transgenic line expressing the β-glucuronidase gene under the control of the 4-kb DNA fragment located immediately upstream of the *DNF2* predicted start codon. ZI, ZII and ZIII correspond to zones I, II and III, respectively. The asterisk and the arrow show infected and noninfected cells, respectively. Bar, 200 µm.

MTR_4g085800 is required for nitrogen fixation

In order to link the *MTR_4g085800* gene mutation with the Fix⁻ phenotype, we analysed 25 plants from the progeny of an NF0217 heterozygous R1 line. Of these 25 plants, six had a Fix⁻ phenotype, indicating that the mutation responsible for the phenotype is recessive. Genotyping of the 25 plants showed co-segregation between NF0217Ase4 homozygote mutants and the Fix⁻ phenotype, indicating that the mutation in *MTR_4g085800* is probably responsible for the Fix⁻ phenotype. In order to further validate the involvement of this putative PI-PLCXD protein in the symbiotic process, we screened our Fix⁻ mutant collection for additional lines harboring insertions in this gene. Two additional mutant lines altered in the same gene were identified by PCR: NF2496 and MS240. These two lines have a *Tnt1* insertion in the third exon (544 bp downstream of the AUG start codon) and a *MERE1* insertion in the sixth exon (1481 bp downstream of the start codon) of *MTR_4g085800*, respectively (Fig. 1a). Backcrosses to WT R108 for the three lines confirmed the recessive character of the mutations. Allelic tests were performed between the three R108 mutant lines NF0217, NF2496 and MS240. Crosses were made as follows: NF0217 was mated with NF2496 and MS240; in addition, MS240 was mated with NF2496. The Jemalong *dnf2* mutant was mated with MS240. For all crosses, the resulting F1 plants (nine for each cross) displayed a Fix⁻ phenotype, proving that the four lines form only one complementation group. These four independent lines altered in *MTR_4g085800* were generated using three distinct mutagenesis protocols in two different genetic backgrounds. Characterization of multiple, independent mutant alleles clearly indicates that mutations in *MTR_4g085800* are responsible for the Fix⁻ phenotype in these lines. Subsequently, Jemalong *dnf2*, NF0217, NF2496 and MS240 were referred to as *dnf2-1*, *dnf2-2*, *dnf2-3* and *dnf2-4*, respectively. The knockout nature of the mutations was evaluated using quantitative reverse transcription-polymerase chain reaction (qRT-PCR). *DNF2* mRNA was not detectable in nodules of *dnf2-2* and *dnf2-4*, indicating that these alleles are knockout mutants. The signal obtained with *dnf2-3* nodules was close to the negative control (Fig. S2).

The phenotypes of the three R108 mutants, *dnf2-2*, *dnf2-3* and *dnf2-4*, were indistinguishable. At the whole-plant level, each line exhibited a typical Fix⁻ phenotype, that is, under symbiotic conditions, the mutants were smaller than WT plants, displayed chlorosis and anthocyanin accumulation, which are commonly associated with nitrogen deficiency (Fig. S3a), and formed more nodules than the WT (Figs 2a, S4). Mutant nodules were smaller and, in contrast with the pink-pigmented WT nodules (Fig. 2a,b), they were either white or brownish (Figs 2a,c,d, S4). Furthermore, as described previously for the Jemalong *dnf2-1* mutant (Mitra & Long, 2004; Starker *et al.*, 2006), the R108 *dnf2-4* mutant does not support either the expression of the bacterial *nifH* gene responsible for nitrogenase production (Fig. S3b, c) or the acetylene reduction activity (Fig. S3d). When grown in nitrogen sufficient conditions, the mutants were identical to the WT (data not shown). Taken together; the genetic analyses
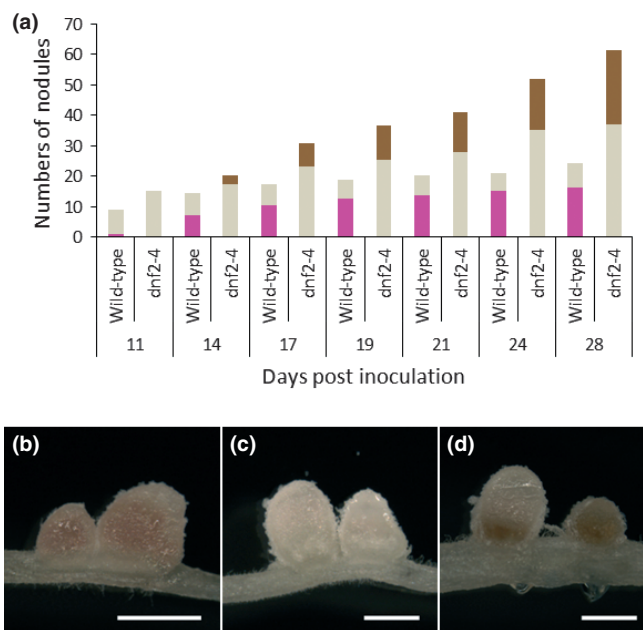

Fig. 2 Brownish nodules are produced in *dnf2*. (a) The total number of nodules developed on *dnf2-4* roots is higher than that on wild-type roots. *Medicago truncatula* wild-type and *dnf2-4* nodules were counted on five pools of nine plants each. White bars, nonfixing nodules; pink bars, N₂-fixing nodules; brown bars, brownish nodules. Note that brownish nodules are present only on the mutant line. (b) Wild-type nodules harvested 18 d post-inoculation (dpi) are pink. (c) 18-dpi *dnf2-4* white nodules. (d) 18-dpi *dnf2-4* nodules that have developed a brownish coloration. Bars: (b) 1 mm; (c, d) 0.5 mm. Similar results were obtained with the other two R108 mutant lines (data not shown).

showed that *MTR_4g085800* corresponds to the *DNF2* symbiotic gene required for effective nitrogen fixation.

DNF2 transcripts are nodule specific, alternatively spliced and accumulate from the infection zone to the distal part of the fixation zone

The MtGEA dataset was generated using *M. truncatula* ecotype Jemalong, whereas the *Tnt1* mutant collection was generated in *M. truncatula* ecotype R108. In order to determine whether the *DNF2* expression profile is similar in R108, relative transcript levels were measured in leaves, stems, petioles, roots and nodules of WT plants by qRT-PCR. Transcripts were detected only in nodules (Fig. 1c), in agreement with data from Jemalong, reported in MtGEA (Fig. 1b). Relative gene expression was detectable in the youngest nodule sample at 6 dpi (Fig. 1c), when pink pigmentation was first visible. Transcript levels were higher at 10 dpi and remained high in mature nodules (Fig. 1c). Remarkably, when sequencing cDNA products, we observed alternative splicing of the *DNF2* gene transcript. Our observations indicate that at least five splice variants exist for the primary *DNF2* transcript. Alternative splicing results in the nonsplicing of the first intron, and in variations in the third exon length (Figs 1a, S5).

In order to gain an insight into the putative *DNF2* function, the expression pattern of *DNF2* was investigated further *in situ*. A genetic construct carrying the β-glucuronidase reporter gene

under the control of the *DNF2* promoter was introduced into *M. truncatula* R108 through *Agrobacterium tumefaciens* transformation to produce transgenic plants. Histological analyses revealed that the cloned fragment activates β-glucuronidase expression from the infection zone to the distal part of the fixation zone (Fig. 1d). Taken together, the data show that *DNF2* is expressed specifically in nodules in the invasion zone and interzone II–III, and that alternative splicing may generate different peptides which may have divergent functional features.

dnf2 nodules have a reduced zone with infected cells and senesce prematurely

In order to determine which steps of the symbiotic process are altered in the mutant, we characterized the structure of *dnf2* nodules. The results presented in Fig. 3 do not reveal any differences between WT and *dnf2* nodules in the meristem and the infection zones (Fig. 3a,b), but highlight striking differences in zones III and IV (Fig. 3e,f). In *dnf2* nodules, the equivalent of WT zone III, which we named zone III*, is properly invaded by the rhizobia at 9 dpi (Fig. 3a,b), but consists of only a few cell layers after 11 dpi (Fig. 3e,f). Furthermore, most infected cells in zone III* have a granular appearance, indicating that the bacteroids in these cells are aberrant (Fig. 3c,d). The senescence zone appeared earlier in *dnf2* nodules than in the WT. Zone IV can be observed as early as 11 dpi in the mutant, when it is still completely absent in WT nodules (Fig. 3e,f). The senescence zone first appeared at *c.* 20 dpi in the WT in our experiments. Consistent with these observations, we found that the expression of a nodule cysteine proteinase senescence marker, TC100437 (*MTR_5g022560*; Van de Velde *et al.*, 2006), was strongly induced, as early as 10 dpi, in *dnf2* relative to WT (Fig. 4a). The differentiation of plant
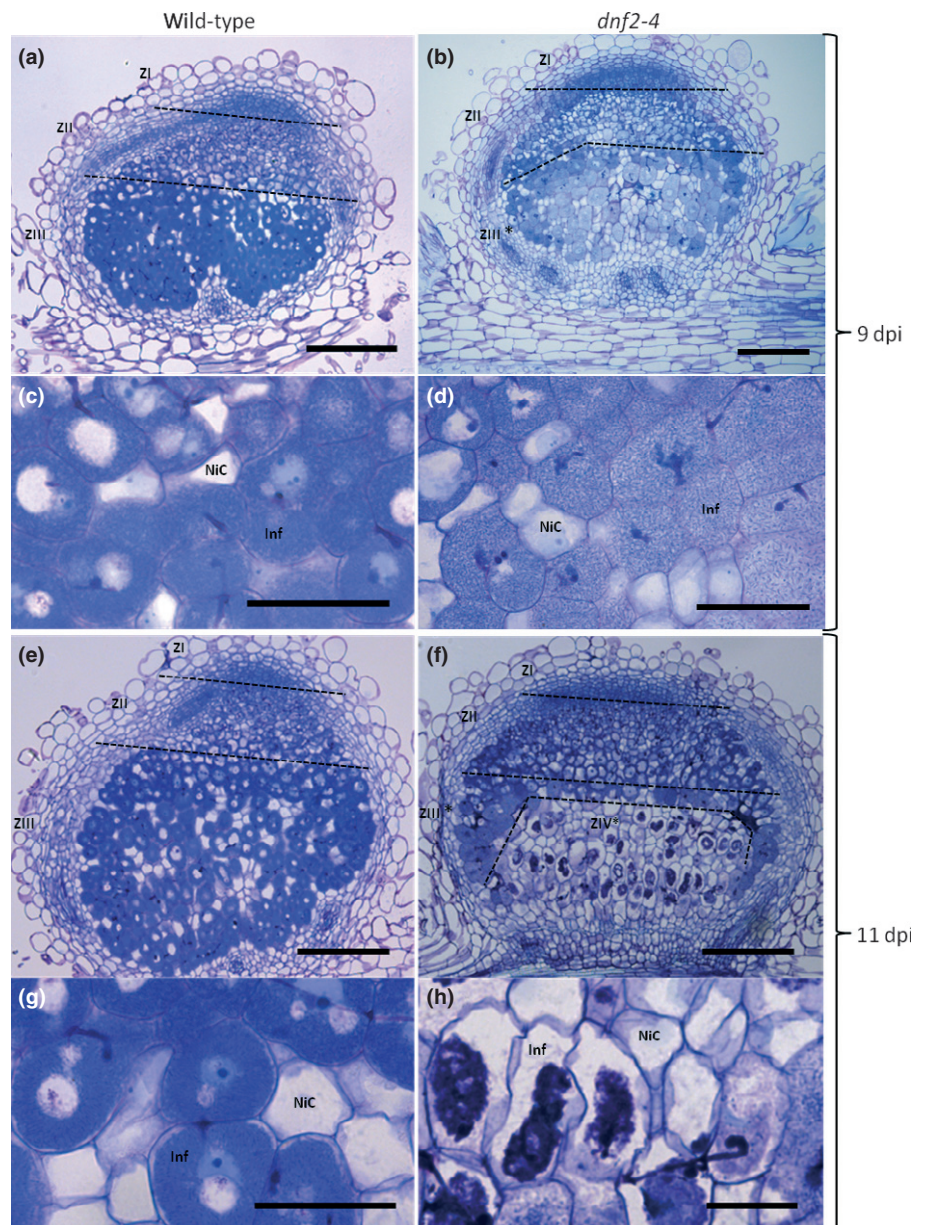

Fig. 3 Modified zonation in *dnf2* nodule. Sections of 9- and 11-d post-inoculation (dpi) nodules of *Medicago truncatula* wild-type and *dnf2-4* plants inoculated with the *Sinorhizobium meliloti* strain Rm41. (a, b, e, f) Sections of entire wild-type nodules (a, e) and *dnf2-4* nodules (b, f). The different zones are delimited by dotted lines. ZI, meristematic zone; ZII, infection zone; ZIII, wild-type fixation zone; ZIII*, modified ZIII present in *dnf2-4* nodules; ZIV*, early senescence zone in *dnf2-4* nodules. (c, d, g, h), enlargements of photographs in (a, b, e, f), respectively. Inf, infected cell; NiC, noninfected cell. Bars: 200 m for enlargements and 50 m for entire nodules. At 9 dpi, the fixation zone is already well developed in wild-type nodules, but not in *dnf2-4* nodules, where fully infected cells are less numerous. Enlargements show 9-dpi wild-type infected cells completely filled with bacteroids, whereas *dnf2-4* infected cells present a granular aspect. At 11 dpi, a senescent zone is present in *dnf2-4*, but not in the wild-type. Enlargement suggests degeneration of the bacteria in *dnf2-4*.
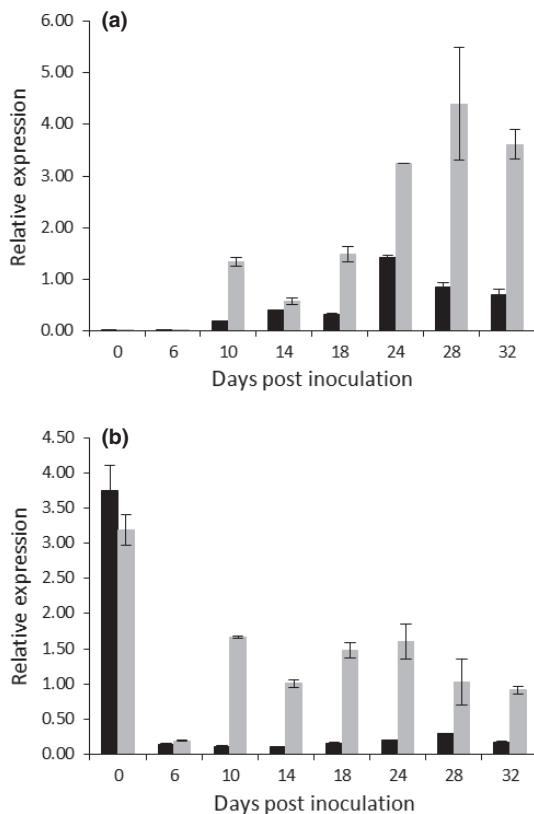
Fig. 4 Upregulation of senescence and defense markers in *dnf2* nodules. TC100437 (a) and TC94217 (b) encode a cysteine proteinase (Van de Velde *et al.*, 2006) and a pathogenesis-related protein 10 (Samac *et al.*, 2011), respectively. Relative transcript levels of these two genes were determined by quantitative reverse transcription-polymerase chain reaction (qRT-PCR) in nodules harvested from *Medicago truncatula* wild-type (black bars) and *dnf2-4* (gray bars) roots after the indicated times expressed as days post-inoculation (dpi). The 'time 0' sample represents a root segment collected immediately after inoculation. Results were normalized using *RBP1*. The error bars represent ± SE; error bars are present on every sample; they are not visible on some bars because of undetectable differences in relative gene expression. Similar expression patterns were obtained for the *dnf2-2* and *dnf2-3* alleles (data not shown).

symbiotic cells, characteristic of a functional nitrogen fixation zone, was investigated using flow cytometry. In agreement with the observed reduced size of zone III (Fig. 3e,f), we observed a drastic reduction in EI in the *dnf2* mutant relative to the WT (Table S2), reflecting a smaller number of differentiated plant cells, and hence the reduced zone III* in *dnf2* nodules. Nevertheless, the presence of a significant number of nodule cells with ploidy levels of 16C, 32C and 64C in *dnf2* (Table S2) indicates that the symbiotic cells had grown to a mature size (Vinardell *et al.*, 2003; Maunoury *et al.*, 2010).

DNF2 is required to produce fully differentiated bacteroids

Light microscopy suggests that the bacteroids within symbiotic cells of *dnf2* nodules are abnormally developed (Fig. 3c,d). In order to determine the effects of the *dnf2* mutation at the ultrastructural level, *dnf2-4* and WT nodules at 24 dpi were observed
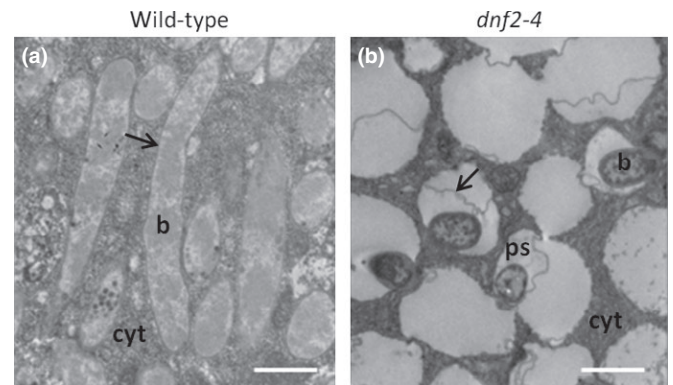

Fig. 5 Enlargement of the peribacteroid space in mutant symbiosomes. Transmission electron microscopy (TEM) images in *Medicago truncatula* wild-type symbiotic cells (a) at 24 d post-inoculation show that bacteroids are elongated and the peribacteroid space is not visible. In infected cells of the *dnf2-4* nodule (b), bacteroids remain small and the peribacteroid space is enlarged. Some symbiosomes seem to be fused. Arrows indicate the symbiosome membrane. b, bacteroid; cyt, cytoplasm; ps, peribacteroid space. Bars, 1.25 μm.

by transmission electron microscopy (TEM; Fig. 5). We could not detect differences between WT and *dnf2-4* nodules in the meristematic region and in the infection zone. By contrast, and in agreement with the light microscopy observations, zone III was drastically modified in the *dnf2-4* mutant. In WT nodules, bacteroids displayed the characteristic elongated shape of differentiated bacteria, reaching > 5 μm in length (Fig. 5a), and completely filling the symbiosomes. In these WT symbiosomes, the peribacteroid space appeared very thin or not visible (Fig. 5a). By contrast, in the mutant nodules, the peribacteroid membrane seemed to be pulled away from the bacteroid, leaving a large peribacteroid space that occupied most of the symbiosome (Fig. 5b). A lack of bacteroid differentiation was confirmed in the *dnf2-4* mutant using flow cytometry and optical microscopy on isolated bacteroids (Fig. S6).

dnf2 mutant nodules display defense-like reactions

Nodules of the three R108 *dnf2* mutants often exhibited dark brown pigmentation in symbiosis with the Rm41 strain (Fig. 2a,d). This was also observed when using Sm1021 (Fig. S4) and Sm2011 (data not shown). Brown pigmentation was visible immediately below the few layers of invaded cells (Fig. 6b) and was never observed in the apical zone. The brown pigments fluoresced green under UV illumination when using a green fluorescent protein (GFP) filter (Fig. 6d), indicating that they may be phenolic compounds. The presence of phenolic compounds in mutant, but not in WT, nodules was confirmed with a potassium permanganate/methylene blue staining procedure (Fig. 6e–h) that detects such compounds (Vasse *et al.*, 1993). Remarkably, brownish nodules were never observed on WT plants, even when senescence had started at 24 dpi (Figs 2a, 4a, S4). Thus, the accumulation of phenolic compounds was not typical of nodule senescence. Because the accumulation of phenolic compounds is often associated with plant defense reactions (Nicholson & Hammerschmidt, 1992), we measured the transcript levels of pathogenesis-related

protein 10 (PR10, TC94217/*MTR_2g035150*; Fig. 4b, Table S1), which is a molecular marker of plant defense (Samac *et al.*, 2011). Elevated levels of *PR10* transcript were found in *dnf2-4* mutant nodules at 10 dpi. By contrast, *PR10* transcript levels remained low in WT, even at 32 dpi (Fig. 4b).

DNF2 is required for bacteroid viability

In view of the evidence for plant defense-like responses and early senescence in *dnf2* nodules, we tested the viability of bacteroids using a staining procedure which allows live and dead bacteria to be distinguished. Using sections of 19-dpi nodules, we found that bacteroids in the fixation zone of WT nodules were mostly alive (Fig. 7a,c), whereas only a few bacteroids in zone III* of *dnf2-4* nodules had intact membranes, as indicated by the green fluorescence of Syto9 (Fig. 7b,d). Bacterial cells in the proximal, brown-pigmented region of *dnf2-4* nodules stained red with propidium iodide, indicating that their membranes were compromised, and hence dead or dying (Fig. 7d). Thus, DNF2 helps to prevent bacterial cell death in infected nodule cells.

Discussion

Here, we have described a new symbiotic gene of *M. truncatula*, *DNF2* (*MTR_4g085800*), that is required for nitrogen fixation, but not for nodule development. Three R108 insertion mutant lines harboring different mutant alleles of this gene were isolated and shown to be allelic to the previously described *dnf2* Jemalong deletion mutant (Mitra & Long, 2004; Starker *et al.*, 2006).

The Jemalong *dnf2* mutant displays no acetylene reduction activity. In addition, this mutant does not support the expression of the bacterial gene, *nifH*, which is required for nitrogen fixation, suggesting that the maintenance of bacteroids may be affected (Starker *et al.*, 2006). Consistent with the observation that *DNF2* is maximally expressed at the onset of nitrogen fixation, our work revealed no differences between *dnf2* and WT until bacteria were released from infection threads. At this stage, and in contrast with WT, rhizobia in *dnf2* nodules do not differentiate into N₂-fixing, fully elongated bacteroids. The electron microscopy study showed that, in the mutant, the peribacteroid space was larger and the bacterial cells remained
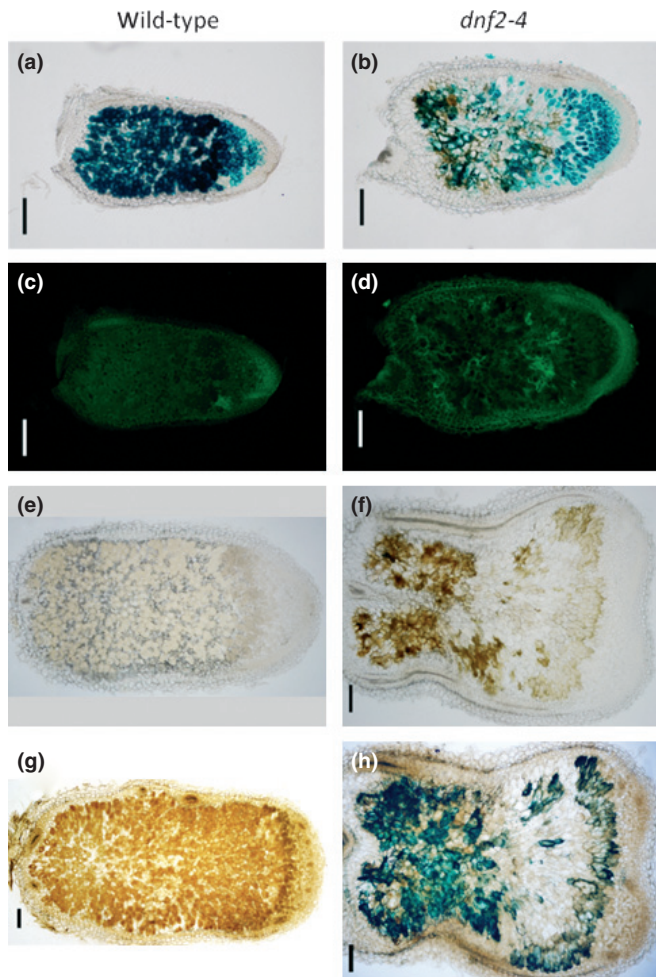

Fig. 6 Accumulation of phenolic compounds in *dnf2* nodules. (a, b) Nodules from wild-type *Medicago truncatula* R108 (a) and *dnf2-4* (b) plants inoculated with the *Sinorhizobium meliloti* strain Sm2011-pXLGD4 carrying the *hemA::LacZ* reporter. Nodules were harvested at 14 d post-inoculation. Glutaraldehyde-fixed nodules were sliced into 50-μm sections and stained with X-Gal to reveal, in blue, the presence of rhizobia constitutively expressing the *LacZ* gene. Sections were then observed using bright-field microscopy. *dnf2-4* nodules present a brown coloration in the central and proximal regions. (c, d) Wild-type (c) and *dnf2-4* (d) nodule sections from (a) and (b) observed under fluorescence illumination using a BrightLine GFP filter set EX47. In *dnf2-4* nodules, brown spots (b) co-localize with green fluorescence (d). (e–h) Sections of unfixed nodules from wild-type (e, g) and *dnf2-4* (f, h) plants inoculated with the *S. meliloti* strain Sm2011-pXLGD4 observed with bright-field microscopy. (e, f) No staining. (g, h) Nodule sections stained with potassium permanganate and methylene blue to reveal the presence of phenolic compounds which stain blue. Bars: (a–d) 200 μm; (e–h) 100 μm.
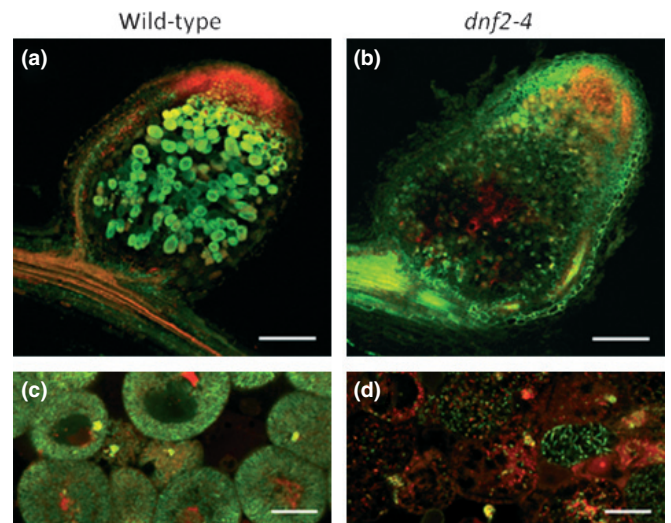

Fig. 7 Reduced viability of bacteroids in *dnf2* nodules. Live/dead staining of nodules from *Medicago truncatula* R108 wild-type (a, c) and *dnf2-4* (b, d) roots inoculated with the *Sinorhizobium meliloti* strain Rm41. Freshly sliced nodules were stained with Syto9 (green signal) and propidium iodide (PI; red signal) and sections were observed using confocal microscopy. Viable bacteroids are stained by Syto9 and dead bacteroids are stained by PI. (c) and (d) represent enlargements of (a) and (b), respectively. Bars: (a, b) 200 μm; (c, d) 50 μm.

small, confirming that they were not differentiated (Fig. 5b). The enlarged peribacteroid space indicates that the peribacteroid membrane is continuously produced in the mutant despite the cessation of bacterial enlargement and differentiation, suggesting that the two processes are disconnected. We also observed that bacteroids lose their viability (Fig. 7b,d) after being released into *dnf2* symbiotic cells, in contrast with WT (Fig. 7a,c), possibly because they are influenced by the toxicity of NCR peptides, as is the bacterial *bacA* mutant (Haag *et al.*, 2011), or because they trigger active defense-like responses in the *dnf2* mutant. Consistent with the loss of bacterial viability, bacteroids appear to be degraded more rapidly, and the nitrogen-fixing zone is replaced by a zone of empty cells containing cellular debris in *dnf2* nodules (Fig. 3e–h).

The cysteine proteinase marker TC100436 is expressed prematurely in the *dnf2* mutant (Fig. 4a), consistent with the early degeneration of infected cells observed in zone III* (Fig. 3). Interestingly, senescence markers, such as cysteine proteinases, are induced in the *L. japonicus sen1* mutant (Suganuma *et al.*, 2004), as well as in ineffective nodules induced by a *nifH::Tn5 S. meliloti* mutant on alfalfa (Barsch *et al.*, 2006). This suggests that senescence reflects a general response of nonfunctional nodules (Maunoury *et al.*, 2010).

The impaired differentiation and bacterial death are correlated with activation of plant defense-like reactions in *dnf2* mutant nodules, as indicated by the expression of the *PR10* defense gene (Fig. 4b) and the accumulation of phenolic compounds (Fig. 6). PR10 induction and necrotic nodules are triggered when inefficient symbiosis results from boron deprivation in *Pisum sativum* and *Phaseolus vulgaris* (Redondo-Nieto *et al.*, 2007). However, this phenotype is not a typical feature of Fix⁻ mutants. Indeed, in the R108 background, the majority of Fix⁻ mutants described in Pislariu *et al.* (2012) do not accumulate these compounds. *dnf2-1* has also been suggested to accumulate phenolic compounds near the infection zone (Pislariu & Dickstein, 2007); thus, defense-like reactions are not likely to be a specific trait of *dnf2* in the R108 background. PR10 gene induction and the accumulation of phenolic compounds were not observed in R108 WT nodules (Figs 4b, 6), even at 32 dpi when late senescent nodules are present, as attested by the induction of the selected senescence marker (Fig. 4a). Furthermore, defense-like reactions were not described in the *L. japonicus sen1* mutant (Suganuma *et al.*, 2004) or in nodules induced by the *nifH* or *nifA* Fix⁻ mutants (Barsch *et al.*, 2006; Maunoury *et al.*, 2010). This supports the idea that, during aborted symbiosis, early senescence is not necessarily associated with defense-like reactions. The *DNF2* gene encodes a PI-PLCXD-containing protein that has homologs in many plant species, including nonlegumes and nonmycorrhized plants, with multiple homologs in each. Although some homologs of DNF2 obviously fulfill roles unrelated to symbiosis, the nodule-specific expression of *DNF2* and the mutant phenotype indicate that the DNF2 PI-PLCXD-containing protein has been recruited to play a specific role in the rhizobium–legume symbiosis with *M. truncatula*. The expression profile of the *DNF2* homolog, *LjNUF* in *L. japonicus* (Kinoshita *et al.*, 2004), suggests that it may play a similar role in the determinate nodule symbiosis.

PI-PLCXD-containing proteins are distinct from *bona fide* eukaryotic phosphatidylinositol-specific phospholipase C proteins (PI-PLCs). PI-PLCs have a multidomain architecture consisting of various regulatory domains and of a PLC catalytic core, which is composed of X and Y regions, separated by a linker. By contrast, PI-PLCXD-containing proteins only contain an X domain (Heinz *et al.*, 1998). A subgroup of PI-PLCXD-containing proteins, which includes DNF2, is found in eukaryotes and in bacteria. These proteins have a similar overall structure, consisting of an N-terminal signal peptide, indicating probable entry of the proteins in the secretory pathway, followed by the PI-PLCXD, and with a total size of 320–420 amino acids. However, the biochemical and biological functions of these proteins remain unclear and, to our knowledge, DNF2 is the first example for which a biological function can be implied based on the phenotype in knockout mutants.

Canonical PI-PLCs cleave phosphatidylinositol (PI) or phosphorylated phosphatidylinositol (PIP) derivatives to produce inositol phosphate and diacylglycerol. These compounds are second messengers or precursors of second messengers, and can participate in plant defense reactions (Canonne *et al.*, 2011). It is difficult to reconcile this with the observed phenotype. As DNF2 does not present all the characteristic domains of eukaryotic PI-PLC, one could consider the possibility that *DNF2* interacts with PI(P) without triggering cleavage. A speculation that could fit with the two observations would be that, by binding to PI(P), DNF2 prevents cleavage. This would result in the repression of defense reactions normally triggered by PI(P) degradation products. In eukaryotes, phosphatidylinositides play important roles in membrane trafficking (Michell, 2011). It is also known that some intracellular bacterial pathogens can produce PI(P)-binding proteins or PI(P)-modifying enzymes to disturb membrane trafficking and to persist inside animal cells (Weber *et al.*, 2009). DNF2 might act in a similar way through phosphatidylinositides to avoid the premature lysis of the symbiosome. It will be interesting to determine whether DNF2 supports bacteroid persistence in plant cells by acting on PI(P), especially given the induction of plant defense-like reactions in the *dnf2* mutants.

The localization of the DNF2 protein will probably contribute to an understanding of its molecular mechanism. Our study has revealed the existence of five mRNA splice variants for *DNF2*. All variants conserved the region coding for the PI-PLCXD. The most abundant transcript, corresponding to TC119183, encodes a signal peptide-containing protein, but additional *DNF2* mRNAs are predicted to generate proteins lacking the signal peptide (Fig. 1a). Putative splice variants of the third exon that include the first intron of a *Phaseolus vulgaris DNF2* homolog are produced in nodules of common bean (Ramirez *et al.*, 2005; Fig. S5). Such a splicing event is not detectable amongst *Arabidopsis* expressed sequence tags (ESTs), suggesting that this phenomenon could be legume specific. The different amino acid sequences of the predicted DNF2 proteins, resulting from the alternative splicing of the primary *DNF2* transcript, indicate that they may be addressed to different compartments of the cell. Some signal peptide-containing proteins that are expressed in symbiotic cells are known to be transported to the symbiosomes

(Liu *et al.*, 2006; Coque *et al.*, 2008; Hohnjec *et al.*, 2009; Van de Velde *et al.*, 2010; Meckfessel *et al.*, 2012). Future studies will be necessary to determine the subcellular location of the different peptides and their capacity to restore the WT phenotype.

Taken together, our results indicate that *DNF2* is necessary for complete differentiation of bacteroids (Figs 5b, S6) and to maintain symbiosomes (Figs 3, 7). Bacterial mutants altered in the nitrogenase structural gene *nifH* or in micro-oxic respiration *fixL* undergo terminal differentiation resulting in fully elongated bacteroids (Maunoury *et al.*, 2010). This indicates that the lack of elongation of bacteroids does not result from an expression defect of *nif* or *fix* genes in *dnf2*, and thus that *dnf2* acts upstream of the establishment of micro-aerobic respiration.

In addition to the bacterial lack of differentiation, mobilization of plant defense-like reactions was observed in the *DNF2* mutants (Figs 4b, 6). It is possible that these phenomena are linked and that incomplete bacteroid differentiation or a defect in symbiosome maintenance in the *dnf2* mutants results from, or triggers, the induction of defense-like reactions. Arguments exist supporting both hypotheses. For instance, the undifferentiated *bacA* bacterial mutant does not trigger plant defense-like reactions. By contrast, only a fraction of the *dnf2* mutant nodules are brownish, suggesting that plant defense-like reactions are only secondary effects of the *DNF2* mutation. Future studies are now required to establish the sequence of events resulting from *DNF2* mutations.

In summary, in this work, we have identified the *DNF2* gene and have further defined its role in the symbiotic process as an actor in symbiosome maintenance. The challenge for future studies will be to determine the molecular function of DNF2 in order to explain its role in the persistence of the symbiosome inside the symbiotic cells.

Acknowledgements

References

Ardourel M, Demont N, Debelle F, Maillet F, de Billy F, Prome JC, Denarie J, Truchet G. 1994. *Rhizobium meliloti* lipooligosaccharide nodulation factors: different structural requirements for bacterial entry into target root hair cells and induction of plant symbiotic developmental responses. *Plant Cell* 6: 1357–1374.

Barsch A, Tellström V, Patschkowski T, Küster H, Niehaus K. 2006. Metabolite profiles of nodulated alfalfa plants indicate that distinct stages of nodule organogenesis are accompanied by global physiological adaptations. *Molecular Plant–Microbe Interactions* 19: 998–1013.

Benedito VA, Torres-Jerez I, Murray JD, Andriankaja A, Allen S, Kakar K, Wandrey M, Verdier J, Zuber H, Ott T *et al.* 2008. A gene expression atlas of the model legume *Medicago truncatula*. *Plant Journal* 55: 504–513.

Boivin C, Camut S, Malpica CA, Truchet G, Rosenberg C. 1990. *Rhizobium meliloti* genes encoding catabolism of trigonelline are induced under symbiotic conditions. *Plant Cell* 2: 1157–1170.

Brocard L, Schultze M, Kondorosi A, Ratet P. 2006. T-DNA mutagenesis in the model plant *Medicago truncatula*: is it efficient enough for legume molecular genetics? *CAB reviews: Perspectives in Agriculture, Veterinary Science, Nutrition and Natural Resources* 1: 1–7.

Canonne J, Froidure-Nicolas S, Rivas S. 2011. Phospholipases in action during plant defense signaling. *Plant Signaling & Behaviour* 6: 13–18.

Cebolla A, Vinardell JM, Kiss E, Olah B, Roudier F, Kondorosi A, Kondorosi E. 1999. The mitotic inhibitor *ccs52* is required for endoreduplication and ploidy-dependent cell enlargement in plants. *EMBO Journal* 18: 4476–4484.

Cheng X, Wen J, Tadege M, Ratet P, Mysore KS. 2011. Reverse genetics in *Medicago truncatula* using *Tnt1* insertion mutants. *Methods in Molecular Biology* 678: 179–190.

Coque L, Neogi P, Pislariu C, Wilson KA, Catalano C, Avadhani M, Sherrier DJ, Dickstein R. 2008. Transcription of *enod8* in *Medicago truncatula* nodules directs *enod8* esterase to developing and mature symbiosomes. *Molecular Plant–Microbe Interactions* 21: 404–410.

Cosson V, Durand P, d'Erfurth I, Kondorosi A, Ratet P. 2006. *Medicago truncatula* transformation using leaf explants. *Methods in Molecular Biology* 343: 115–127.

Ehrhardt DW, Atkinson EM, Long SR. 1992. Depolarization of alfalfa root hair membrane potential by *Rhizobium meliloti* nod factors. *Science* 256: 998–1000.

El Yahyaoui F, Kuster H, Ben Amor B, Hohnjec N, Puhler A, Becker A, Gouzy J, Vernie T, Gough C, Niebel A *et al.* 2004. Expression profiling in *Medicago truncatula* identifies more than 750 genes differentially expressed during nodulation, including many potential regulators of the symbiotic program. *Plant Physiology* 136: 3159–3176.

d'Erfurth I, Cosson V, Eschstruth A, Lucas H, Kondorosi A, Ratet P. 2003. Efficient transposition of the *Tnt1* tobacco retrotransposon in the model legume *Medicago truncatula*. *Plant Journal* 34: 95–106.

Garcia J, Barker DG, Journet EP. 2006. Seed storage and germination. In: Mathesius U, Journet EP, Sumner LW, eds. *The Medicago truncatula handbook*. ISBN 0-9754303-1-9. URL: http://www.noble.org/MedicagoHandbook/

Haag AF, Baloban M, Sani M, Kerscher B, Pierre O, Farkas A, Longhi R, Boncompagni E, Herouart D, Dall'angelo S *et al.* 2011. Protection of *Sinorhizobium* against host cysteine-rich antimicrobial peptides is critical for symbiosis. *PLoS Biology* 9: e1001169.

Hakoyama T, Niimi K, Watanabe H, Tabata R, Matsubara J, Sato S, Nakamura Y, Tabata S, Jichun L, Matsumoto T *et al.* 2009. Host plant genome overcomes the lack of a bacterial gene for symbiotic nitrogen fixation. *Nature* 462: 514–517.

Hakoyama T, Niimi K, Yamamoto T, Isobe S, Sato S, Nakamura Y, Tabata S, Kumagai H, Umehara Y, Brossuleit K *et al.* 2012. The integral membrane protein SEN1 is required for symbiotic nitrogen fixation in *Lotus japonicus* nodules. *Plant and Cell Physiology* 53: 225–236.

Hardy RWF, Holsten RD, Jackson EK, Burns RC. 1968. The acetylene-ethylene assay for N$_2$ fixation: laboratory and field evaluation. *Plant Physiology* 43: 1185–1207.

He J, Benedito VA, Wang M, Murray JD, Zhao PX, Tang Y, Udvardi MK. 2009. The *Medicago truncatula* gene expression atlas web server. *BMC Bioinformatics* 10: 441.

Heinz DW, Essen LO, Williams RL. 1998. Structural and mechanistic comparison of prokaryotic and eukaryotic phosphoinositide-specific phospholipases C. *Journal of Molecular Biology* 275: 635–650.

Hoffmann B, Trinh TH, Leung J, Kondorosi A, Kondorosi E. 1997. A new *Medicago truncatula* line with superior *in vitro* regeneration, transformation, and symbiotic properties isolated through cell culture selection. *Molecular Plant–Microbe Interactions* 10: 307–315.

Hohnjec N, Lenz F, Fehlberg V, Vieweg MF, Baier MC, Hause B, Küster H. 2009. The signal peptide of the *Medicago truncatula* modular nodulin Mtnod25 operates as an address label for the specific targeting of proteins to nitrogen-fixing symbiosomes. *Molecular Plant–Microbe Interactions* 22: 63–72.

Iantcheva A, Chabaud M, Cosson V, Barascud M, Schutz B, Primard-Brisset C, Durand P, Barker DG, Vlahova M, Ratet P. 2009. Osmotic shock improves *Tnt1* transposition frequency in *Medicago truncatula* cv jemalong during *in vitro* regeneration. *Plant Cell Reporter* 28: 1563–1572.

Kinoshita N, Ooki Y, Deguchi Y, Chechetka SA, Kouchi H, Umehara Y, Izui K, Hata S. 2004. Cloning and expression analysis of a *mapkkk* gene and a novel nodulin gene of *Lotus japonicus*. *Bioscience Biotechnologies Biochemistry* 68: 1805–1807.

Kondorosi E, Banfalvi Z, Kondorosi A. 1984. Physical and genetic analysis of a symbiotic region of *Rhizobium meliloti*: identification of nodulation genes. *Molecular and General Genetics* 193: 445–452.

Krall L, Wiedemann U, Unsin G, Weiss S, Domke N, Baron C. 2002. Detergent extraction identifies different Virb protein subassemblies of the type IV secretion machinery in the membranes of *Agrobacterium tumefaciens*. *Proceedings of the National Academy of Sciences, USA* 99: 11405–11410.

Kumagai H, Hakoyama T, Umehara Y, Sato S, Kaneko T, Tabata S, Kouchi H. 2007. A novel ankyrin-repeat membrane protein, IGN1, is required for persistence of nitrogen-fixing symbiosis in root nodules of *Lotus japonicus*. *Plant Physiology* 143: 1293–1305.

Lelandais-Briere C, Naya L, Sallet E, Calenge F, Frugier F, Hartmann C, Gouzy J, Crespi M. 2009. Genome-wide *Medicago truncatula* small RNA analysis revealed novel microRNAs and isoforms differentially regulated in roots and nodules. *Plant Cell* 21: 2780–2796.

Leong SA, Williams PH, Ditta GS. 1985. Analysis of the 5' regulatory region of the gene for delta-aminolevulinic acid synthetase of *Rhizobium meliloti*. *Nucleic Acids Research* 13: 5965–5976.

Liu J, Miller SS, Graham M, Bucciarelli B, Catalano CM, Sherrier DJ, Samac DA, Ivashuta S, Fedorova M, Matsumoto P *et al.* 2006. Recruitment of novel calcium-binding proteins for root nodule symbiosis in *Medicago truncatula*. *Plant Physiology* 141: 167–177.

Maunoury N, Redondo-Nieto M, Bourcy M, Van de Velde W, Alunni B, Laporte P, Durand P, Agier N, Marisa L, Vaubert D *et al.* 2010. Differentiation of symbiotic cells and endosymbionts in *Medicago truncatula* nodulation are coupled to two transcriptome-switches. *PLoS ONE* 5: e9519.

Meade HM, Long SR, Ruvkun GB, Brown SE, Ausubel FM. 1982. Physical and genetic characterization of symbiotic and auxotrophic mutants of *Rhizobium meliloti* induced by transposon *Tn5* mutagenesis. *Journal of Bacteriology* 149: 114–122.

Meckfessel MH, Blancaflor EB, Plunkett M, Dong Q, Dickstein R. 2012. Multiple domains in Mtnod8 protein including the signal peptide target it to the symbiosome. *Plant Physiology* 159: 299–310.

Mergaert P, Uchiumi T, Alunni B, Evanno G, Cheron A, Catrice O, Mausset AE, Barloy-Hubler F, Galibert F, Kondorosi A *et al.* 2006. Eukaryotic control on bacterial cell cycle and differentiation in the *Rhizobium*–legume symbiosis. *Proceedings of the National Academy of Sciences, USA* 103: 5230–5235.

Michell RH. 2011. Inositol and its derivatives: their evolution and functions. *Advances in Enzyme Regulation* 51: 84–90.

Mitra RM, Long SR. 2004. Plant and bacterial symbiotic mutants define three transcriptionally distinct stages in the development of the *Medicago truncatula/Sinorhizobium meliloti* symbiosis. *Plant Physiology* 134: 595–604.

Moreau S, Verdenaud M, Ott T, Letort S, de Billy F, Niebel A, Gouzy J, de Carvalho-Niebel F, Gamas P. 2011. Transcription reprogramming during root nodule development in *Medicago truncatula*. *PLoS ONE* 6: e16463.

Nicholson RL, Hammerschmidt R. 1992. Phenolic compounds and their role in disease resistance. *Annual Review of Phytopathology* 30: 369–389.

Oldroyd G. ED, Murray JD, Poole PS, Downie JA. 2011. The rules of engagement in the legume–rhizobial symbiosis. *Annual Review of Genetics* 45: 119–144.

Orosz L, Svab Z, Kondorosi A, Sik T. 1973. Genetic studies on rhizobiophage 16–3. I. Genes and functions on the chromosome. *Molecular General Genetics* 125: 341–350.

Penmetsa RV, Cook DR. 1997. A legume ethylene-insensitive mutant hyperinfected by its rhizobial symbiont. *Science* 275: 527–530.

Pislariu CI, Dickstein R. 2007. An IRE-like AGC kinase gene, *MtIRE*, has unique expression in the invasion zone of developing root nodules in *Medicago truncatula*. *Plant Physiology* 144: 682–694.

Pislariu CI, Murray J, Wen J, Cosson V, Duvvuru Muni RR, Wang M, Benedito V, Andriankaja A, Cheng X, Torres Jerez I *et al.* 2012. A *Medicago truncatula* tobacco-retrotransposon (*Tnt1*)-insertion mutant collection with defects in nodule development and symbiotic nitrogen fixation. *Plant Physiology* 159: 1686–1699.

Rakocevic A, Mondy S, Tirichine L, Cosson V, Brocard L, Iantcheva A, Cayrel A, Devier B, Abu El-Heba GA, Ratet P. 2009. *MERE1, a low-copy-number copia-type retroelement in Medicago truncatula* active during tissue culture. *Plant Physiology* 151: 1250–1263.

Ramirez M, Graham MA, Blanco-Lopez L, Silvente S, Medrano-Soto A, Blair MW, Hernandez G, Vance CP, Lara M. 2005. Sequencing and analysis of common bean ESTs. Building a foundation for functional genomics. *Plant Physiology* 137: 1211–1227.

Redondo-Nieto M, Pulido L, Reguera M, Bonilla I, Bolanos L. 2007. Developmentally regulated membrane glycoproteins sharing antigenicity with rhamnogalacturonan II are not detected in nodulated boron deficient *Pisum sativum*. *Plant, Cell & Environment* 30: 1436–1443.

Rosenberg C, Boistard P, Denarie J, Casse-Delbart F. 1981. Genes controlling early and late functions in symbiosis are located on a megaplasmid in *Rhizobium meliloti*. *Molecular General Genetics* 184: 326–333.

Samac DA, Penuela S, Schnurr JA, Hunt EN, Foster-Hartnett D, Vandenbosch KA, Gantt JS. 2011. Expression of coordinately regulated defence response genes and analysis of their role in disease resistance in *Medicago truncatula*. *Molecular Plant Pathology* 12: 786–798.

Scholte M, d'Erfurth I, Rippa S, Mondy S, Cosson V, Durand P, Breda C, Trinh H, Rodriguez-Llorente I, Kondorosi E *et al.* 2002. T-DNA tagging in the model legume *Medicago truncatula* allows efficient gene discovery. *Molecular Breeding* 10: 203–215.

Starker CG, Parra-Colmenares AL, Smith L, Mitra RM, Long SR. 2006. Nitrogen fixation mutants of *Medicago truncatula* fail to support plant and bacterial symbiotic gene expression. *Plant Physiology* 140: 671–680.

Suganuma N, Yamamoto A, Itou A, Hakoyama T, Banba M, Hata S, Kawaguchi M, Kouchi H. 2004. cDNA macroarray analysis of gene expression in ineffective nodules induced on the *Lotus japonicus sen1* mutant. *Molecular Plant–Microbe Interactions* 17: 1223–1233.

Tadege M, Wen J, He J, Tu H, Kwak Y, Eschstruth A, Cayrel A, Endre G, Zhao PX, Chabaud M *et al.* 2008. Large-scale insertional mutagenesis using the *Tnt1* retrotransposon in the model legume *Medicago truncatula*. *Plant Journal* 54: 335–347.

Timmers AC, Auriac MC, Truchet G. 1999. Refined analysis of early symbiotic steps of the *Rhizobium–Medicago* interaction in relationship with microtubular cytoskeleton rearrangements. *Development* 126: 3617–3628.

Timmers AC, Soupene E, Auriac MC, de Billy F, Vasse J, Boistard P, Truchet G. 2000. Saprophytic intracellular rhizobia in alfalfa nodules. *Molecular Plant–Microbe Interactions* 13: 1204–1213.

Van de Velde W, Guerra JC, De Keyser A, De Rycke R, Rombauts S, Maunoury N, Mergaert P, Kondorosi E, Holsters M, Goormachtig S. 2006. Aging in legume symbiosis. A molecular view on nodule senescence in *Medicago truncatula*. *Plant Physiology* 141: 711–720.

Van de Velde W, Zehirov G, Szatmari A, Debreczeny M, Ishihara H, Kevei Z, Farkas A, Mikulass K, Nagy A, Tiricz H *et al.* 2010. Plant peptides govern terminal differentiation of bacteria in symbiosis. *Science* 327: 1122–1126.

Vasse J, de Billy F, Camut S, Truchet G. 1990. Correlation between ultrastructural differentiation of bacteroids and nitrogen fixation in alfalfa nodules. *Journal of Bacteriology* 172: 4295–4306.

Vasse J, de Billy F, Truchet G. 1993. Abortion of infection during the *Rhizobium meliloti*–alfalfa symbiotic interaction is accompanied by a hypersensitive reaction. *The Plant Journal* 4: 555–566.

Vinardell JM, Fedorova E, Cebolla A, Kevei Z, Horvath G, Kelemen Z, Tarayre S, Roudier F, Mergaert P, Kondorosi A *et al.* 2003. Endoreduplication mediated by the anaphase-promoting complex activator *ccs52a* is required for symbiotic cell differentiation in *Medicago truncatula* nodules. *Plant Cell* 15: 2093–2105.

Wang D, Griffitts J, Starker C, Fedorova E, Limpens E, Ivanov S, Bisseling T, Long S. 2010. A nodule-specific protein secretory pathway required for nitrogen-fixing symbiosis. *Science* 327: 1126–1129.

Weber SS, Ragaz C, Hilbi H. 2009. Pathogen trafficking pathways and host phosphoinositide metabolism. *Molecular Microbiology* 71: 1341–1352.

Welchen E, Gonzalez DH. 2005. Differential expression of the Arabidopsis cytochrome c genes *cytc-1* and *cytc-2*. Evidence for the involvement of tcp-domain protein-binding elements in anther- and meristem-specific expression of the *cytc-1* gene. *Plant Physiology* 139: 88–100.

Young ND, Debelle F, Oldroyd GE, Geurts R, Cannon SB, Udvardi MK, Benedito VA, Mayer KF, Gouzy J, Schoof H *et al.* 2011. The *Medicago* genome provides insight into the evolution of rhizobial symbioses. *Nature* 480: 520–524.

Supporting Information

Additional supporting information may be found in the online version of this article.

Fig. S1 *Medicago truncatula* DNF2 is a conserved protein containing a phosphatidylinositol-specific phospholipase C X domain.

Fig. S2 *Medicago truncatula dnf2-2, dnf2-3* and *dnf2-4* mutants are strongly altered in *DNF2* expression.

Fig. S3 *dnf2* is required to support *nifH* expression and nitrogen fixation.

Fig. S4 Occurrence of brownish nodules in *dnf2* mutants elicited by *Sinorhizobium meliloti* Rm41 or Sm1021 strains.

Fig. S5 *DNF2* is alternatively spliced in legume plants.

Fig. S6 Impairment of bacteroid differentiation in *dnf2* nodules.

Table S1 Primers used in this study

Table S2 *dnf2* nodule cells have a reduced endoreduplication index

Please note: Wiley-Blackwell are not responsible for the content or functionality of any supporting information supplied by the authors. Any queries (other than missing material) should be directed to the *New Phytologist* Central Office.